Joint Torque Analysis of Push Recovery Motions during Human Walking*

R. Malin Schemschat[1], Debora Clever[1], Martin L. Felis[1], Enrico Chiovetto[2], Martin Giese[2], Katja Mombaur[1]

***Abstract*— Most of their lifetime humans can recover from disturbances during walking motions very well. Our assumption is that to recover from disturbances during walking requires higher internal torques in the joints than motions without disturbances. To measure the internal joint torques in experiments is complicated and expensive. In this work we propose an optimality based simulation environment that allows to determine the internal torques in the joints of a human during disturbed walking motions. The human is represented by a two dimensional (2D) rigid multi-body model consisting of 14 segments controlled by torques in 13 rotational joints resulting in 16 degrees of freedom (DoF). The disturbance is modeled as external force acting on the model. A least-squares optimal control problem that minimizes the distance between the joint angles of the model and joint angles gained from motion capture experiments, while satisfying the dynamics and constraints of the human model, is set up. The analysis of perturbed and unperturbed walking motions shows that the torques in the joints vary according to the strength and duration of the disturbance. The calculation of the internal joint torques is important for the development of new control strategies or set up of humanoid robots and prostheses. It can also be used in the context of sport sciences to improve training or therapies.**

I. INTRODUCTION

Undisturbed motion barely exists in real world. In everyday life dangers lurk everywhere. In the usual environment the floor is not exactly plane. Uneven terrain can result in a disturbance of the motion. Walking in crowded places, it can always happen that one is pushed by the fellow human beings. Usually humans can adapt very well to unforeseen perturbations during gait. They are able to recover from the disturbance and carry on walking as long as the push is not too strong. For elderly people walking often becomes less stable and to capture from disturbances can become a hard challenge. The problem of enabling technical assistive devices such as prostheses or exoskeletons to react on perturbations and prevent humans from falling is a future leading field of research. Also for robots it is still a huge challenge to recover even from small pushes. To be able to transfer the ability of humans to recover from perturbations, it is important to get a better understanding of the human motion. Therefore we consider data of human walking motions including the force and the direction of the perturbation from motion capture experiments of one subject, see Figure 1. In [17] a list of the typical approaches on how to handle disturbances during standing, such as the ankle, the hip and the stepping strategy, is given. In [20] these strategies are applied to a robot. For this approach force sensors and a full body model of the robot is needed to calculate the joint torques required to compensate the external disturbance force.

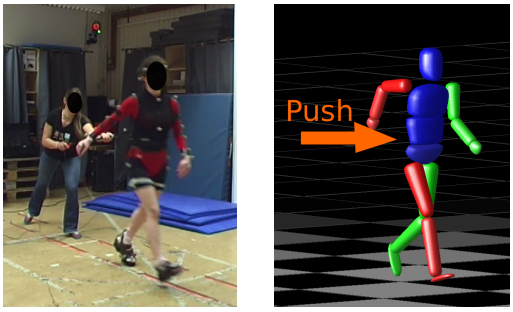

Fig. 1: Motion capture experiments of disturbed human walking motions (left) and a visualization of the motion with our human model in sagittal plane (right).

Even if the determination of joint torques is essential for the analysis of human walking and push recovery motions, the approaches found in literature are rare. Hwang made investigations to evaluate the joint torques in the lower limb (hip and knee joint) during gait using torque sensors of an exoskeleton robot [12]. In [15] the joint torque in the human knee during level ground walking is compared to torques in a knee prosthesis. Wit and Czaplicki determine the joint muscle torques during walking motions in [19]. In [18], Tu and Lee use a two-link manipulator approach to calculate the joint torque during walking on various grounds.

In this paper we regard pushes from the back which vary in strength and in the height of the point at the spine where the push is applied (push point). The resulting motions could be described by a two dimensional rigid multi-body human model. Our approach allows the analysis of the internal torques appearing in the joints during a motion. The gained results find three main application fields: The human motion analysis can be applied in the sport sciences to develop new training strategies. Motions that result in better joint protection can be determined. This can also be helpful in the

*This work was supported by HGS MathComp, University of Heidelberg. Furthermore, the research leading to these results has received funding from the European Union Seventh Framework Program (FP7/2007 - 2013) under grant agreement n° 611909 (KoroiBot).

[1] Optimization in Robotics and Biomechanics, Interdisciplinary Center for Scientific Computing, Heidelberg University, Germany {malin.schemschat, debora.clever, martin.felis, katja.mombaur}@iwr.uni-heidelberg.de

[2] Section for Computational Sensomotorics, Department of Cognitive Neurology, Hertie Institute for Clinical Brain Research, Centre for Integrative Neuroscience, University Clinic Tübingen, Tübingen, Germany {enrico.chiovetto@klinikum.uni-tuebingen.de, martin.giese@uni-tuebingen.de

field of medicine. Better cure therapies could be developed. In the field of prosthetics, exoskeletons and humanoid robots the knowledge of the amount of internal joint torques is important for the development of new technologies, but also for the improvement of old ones. An estimation of the amount of power, a motor of a human-like device needs, can be determined by our approach. Extracting relevant quantities from the model, our approach can also be useful to determine new control strategies for push-recovery motions or disturbance detection.

The purpose of this paper is to propose an optimality based simulation environment to derive the internal torques in the joints during disturbed human walking motions. To gain these torques we use a two dimensional rigid multi-body human model described by differential equations of motions including the disturbance as external force. A least-squares optimal control problem (OCP) is formulated to fit this model to the recorded disturbed human walking motions. As the model is controlled by the internal joint torques, the solution of this OCP gives information about the internal joint torques required for the motion. A similar approach has been made in [10] for undisturbed human motions.

The paper is organized as follows. Section II is divided in four parts: First the human model is described, then the optimal control problem and its solution is presented and in the last part the generation of the reference data by motion capture experiments is described. In Section III the numerical results for five different disturbed and two undisturbed human walking motions are presented. In the last Section IV we give some conclusions and perspectives for future work.

II. METHODS

For our analysis of human push recovery motions, the human is represented by a dynamical multi-body system that allows to include external forces representing the disturbance. We define a least-squares optimal control problem to fit our model to data from motion capture experiments. A description of the model, the optimization tools and the generation of the reference data is given in this section.

A. Model

In this section the multi-body model which is able to represent the dynamics of human push recovery motions is described.

A similar model to the model used in this paper has already been presented in [16]. It is a multi-body system in the sagittal plane that consists of 14 segments connected by 13 joints that enable rotations around the y-axis. The locations of the joints are shown in Figure 2. To allow for movements of the whole body in space, the pelvis is modeled as a floating base that enables translation in the z- and x-directions and rotations around the y-axis. In total the model has 16 degrees of freedom and is described by 32 state variables, consisting of all position and velocity variables. The motion is controlled by 13 control variables, representing the internal torques in the joints.

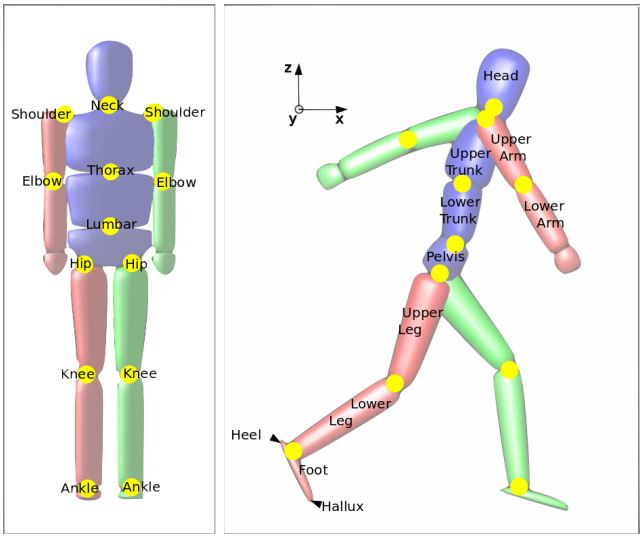

Fig. 2: The two dimensional rigid multi-body human model visualized with MeshUp [9] from different perspectives and the definition of the joints and segments. The joints are marked by yellow dots.

The model used in this work is implemented in the rigid body dynamics library `RBDL` [8]. It is based on the `HeiMan` model [11], a highly parametrized rigid multi-body model for humans. The human body is approximated by a system of rigid bodies connected by rotational joints. Usually four phases are distinguished describing a human step. They are defined by the change of contacts with the ground, [7]. The dynamics of the model can be described by the following differential equation of motion

$$\mathbf{M}(\mathbf{q})\ddot{\mathbf{q}} + \mathbf{C}(\mathbf{q},\dot{\mathbf{q}}) = \boldsymbol{\tau}. \tag{1}$$

Pelvis position and orientation and the joint angles are defined by the vector $\mathbf{q} = (q^{(1)},\dots,q^{(n_q)})$, $q^{(i)} : \mathbb{R} \to \mathbb{R}$, $i = 1,\dots,n_q$, with n_q being the number of degrees of freedom. Analogously $\dot{\mathbf{q}}$ defines the corresponding velocities and $\ddot{\mathbf{q}}$ the accelerations. The joint torques are described by the vector $\boldsymbol{\tau} = (0,0,0,\tilde{\boldsymbol{\tau}}^T)^T \in \mathbb{R}^{n_q}$, where the first three entries correspond to the free floating body. Note, that in the context of optimal control the control vector is defined by the $n_q - 3$ elements of the torque vector which correspond to the actuated joints $\tilde{\boldsymbol{\tau}}$. The inertia term is described by the symmetric and positive definite matrix $\mathbf{M}$ depending also on the joint angles. The vector of functions $\mathbf{C}(\mathbf{q},\dot{\mathbf{q}})$ describes the amount of forces that has to be applied such that the acceleration $\ddot{\mathbf{q}}$ is zero. This term includes the Coriolis and gravity as well as centrifugal and friction forces. For the simulation of contacts, additional constraint equations

$$\mathbf{g}(\mathbf{q}) = 0 \tag{2}$$

have to be fulfilled. They describe the difference between a point and its desired position. To include these conditions equation (1) is changed to

$$\mathbf{M}(\mathbf{q})\ddot{\mathbf{q}} + \mathbf{C}(\mathbf{q},\dot{\mathbf{q}}) = \boldsymbol{\tau} + \mathbf{G}(\mathbf{q})^T\boldsymbol{\lambda}, \tag{3}$$

where $\boldsymbol{\lambda} \in \mathbb{R}^m$ are the constraint forces resulting from a contact ($m =$ number of constraint equations) and $\mathbf{G}(\mathbf{q}) := \frac{\partial}{\partial \mathbf{q}}\mathbf{g}(\mathbf{q})$ is the Jacobi Matrix of the constraints depending on the vector of functions $\mathbf{q}$.

By differentiation of the constraints $\mathbf{g}(\mathbf{q}) = 0$, equation (3) can be formulated as a linear system with the unknowns $\ddot{\mathbf{q}}$ and $\boldsymbol{\lambda} \in \mathbb{R}^m$:

$$\begin{pmatrix} \mathbf{M} & \mathbf{G}^T \\ \mathbf{G} & \mathbf{0} \end{pmatrix} \begin{pmatrix} \ddot{\mathbf{q}} \\ -\boldsymbol{\lambda} \end{pmatrix} = \begin{pmatrix} -\mathbf{C} + \boldsymbol{\tau} \\ -\dot{\mathbf{G}}\dot{\mathbf{q}} \end{pmatrix}. \tag{4}$$

It has to be ensured that the constraints $\mathbf{g}(\mathbf{q}) = 0$ are satisfied at the beginning. After that they are fulfilled on acceleration level.

In our model there are two sources of external forces acting on the model. One is the ground reaction force which is described by constraint forces. In our model the contact of the feet with the ground during a step is represented by two contact points per foot: one in each heel and one in each hallux. In total there are four contact points for the ground contact.

The other source is the disturbance of the motion simulated as an external force acting on the model. For the simulation for the disturbances a fifth contact point is added to the model at three different locations at the spine. The Jacobian of the push point $\mathbf{G}_{\text{push}}$ is calculated. Combined with the applied force $\mathbf{f}_{\text{push}}$ it is included into the model by adding it to the torques in the joints

$$\boldsymbol{\tau} \longmapsto \boldsymbol{\tau} + \mathbf{G}_{\text{push}}^T \mathbf{f}_{\text{push}}.$$

The constraints and right hand sides of the differential equation describing the dynamics of the model are changing during a gait cycle.

B. Optimal Control

To fit the model to the recorded push recovery motions, an optimal control problem is defined:

$$\min_{\mathbf{x},\mathbf{u},\mathbf{p}} \sum_{j=1}^{n_{ph}} \int_{t_{j-1}}^{t_j} \phi_j(\mathbf{x}(t), \mathbf{u}(t), \mathbf{p}) dt \tag{5}$$

$$\text{s.t. } \dot{\mathbf{x}}(t) = \mathbf{f}_j(t, \mathbf{x}(t), \mathbf{u}(t), \mathbf{p}), \text{ for } t \in [t_{j-1}, t_j], \tag{6}$$
$$j = 1, \ldots, n_{ph},\ t_0 = 0, t_{n_{ph}} = T,$$

$$\mathbf{x}(t_j^+) = \mathbf{x}(t_j^-) + J(t_j^-, \mathbf{x}(t_j^-), \mathbf{p}), \tag{7}$$
$$j = 1, \ldots, n_{ph},$$

$$\mathbf{g}_j(t, \mathbf{x}(t), \mathbf{u}(t), \mathbf{p}) \geq \mathbf{0}, \text{ for } t \in [t_{j-1}, t_j], \tag{8}$$

$$\mathbf{r}_{eq}(\mathbf{x}(t_0), \ldots, \mathbf{x}(t_{n_{ph}}), \mathbf{p}) = \mathbf{0}, \tag{9}$$

$$\mathbf{r}_{ineq}(\mathbf{x}(t_0), \ldots, \mathbf{x}(t_{n_{ph}}), \mathbf{p}) \geq \mathbf{0}, \tag{10}$$

where $\mathbf{x} = (x^{(1)}, \ldots, x^{(n_x)}), x^{(i)} : [0,T] \to \mathbb{R}, i = 1, \ldots, n_x$ defines the states (in this paper, positions $\mathbf{q}$ and velocities $\dot{\mathbf{q}}$), $\mathbf{u} = (u^{(1)}, \ldots, u^{(n_u)}), u^{(i)} : [0,T] \to \mathbb{R}, i = 1, \ldots, n_u$ the controls (in this paper, internal joint torques $\tilde{\boldsymbol{\tau}}$), and $\mathbf{p} \in \mathbb{R}^{n_p}$ are parameters. The variable t defines the continuous time variable, $t_0 = 0$ the initial and $t_{n_{ph}} = T$ the final time. The transition times between the n_{ph} phases are given by t_j for $j = 1, \ldots, n_{ph} - 1$. The right hand side of the differential equation in phase j is denoted by $\mathbf{f}_j$. In our case the right hand side (equation (6)) is defined by the equation of motion describing the dynamics of the model described in Section II-A. For each phase initial, final and coupled conditions can be formulated. They are defined in the vector of functions $\mathbf{r}_{eq}$ and $\mathbf{r}_{ineq}$. Other equality and inequality constraints are described by the vector of functions $\mathbf{g}_j$. The contacts of the feet with the ground are defined by the equations (8)-(10).

An objective function for equation (5), that minimizes the distance between the joint angles $\tilde{\mathbf{q}}$ from the reference data and the joint angle $\mathbf{q}$ from the model, is defined as a weighted difference between these angles:

$$\phi(\mathbf{x}(t), \mathbf{u}(t), \mathbf{p}) = \sum_{k=0}^{n_q} \omega_k (q_k(t) - \tilde{q}_k(t))^2 \tag{11}$$

$$+ 0.01 \mathbf{u}(t)^T \mathbf{W}_u \mathbf{u}(t). \tag{12}$$

A further criterion which is a suitably weighted minimization of all squared joint torques is added for regularization (12).

In this paper the phase transition times $t_1, \ldots, t_{n_{ph}}$ are fixed to values suitable for the reference data.

C. Solution Strategy

To solve the resulting optimal control problem, we rely on a direct multiple shooting approach for the discretization coupled with an efficient sequential quadratic programming (SQP) method for the optimization, [5], implemented in the software package `MUSCOD-II` of the Interdisciplinary Center for Scientific Computing, Heidelberg University, [14].

More precisely, the phases of the hybrid system are divided into smaller subintervals, specifying the multiple shooting nodes. By piecewise discretization of the controls and parametrization of the states using a Runge-Kutta scheme, the infinite dimensional problem is reformulated as a discrete nonlinear program (NLP), which is solved by a structure exploiting SQP method, [5].

D. Reference Data

For our approach of the analysis of human push recovery motions reference data is needed. In this work we fit to the joint angles to compute a motion of our model that is as close as possible to the reference data while fulfilling the constraints of the model. The generation of this data is described in this section.

The motion capture data were recorded in the motion capture lab at CIN in Tübingen. An overview of the generation of the motion capture data is shown in Figure 3. A Vicon (Oxfor, UK, [4]) motion capture systems made of 10 infrared cameras was used to record whole-body motion kinematics. The systems tracked the spatial positions of 42 reflective markers with high spatial resolution (error below 1.5 mm). The markers were attached with double-sided adhesive tape to tight clothing worn by the participants. Markers were placed on the locations specified by the Vicons PlugInGait marker set. A Vicon system is used to detect markers a person is wearing on predefined points on the body. The

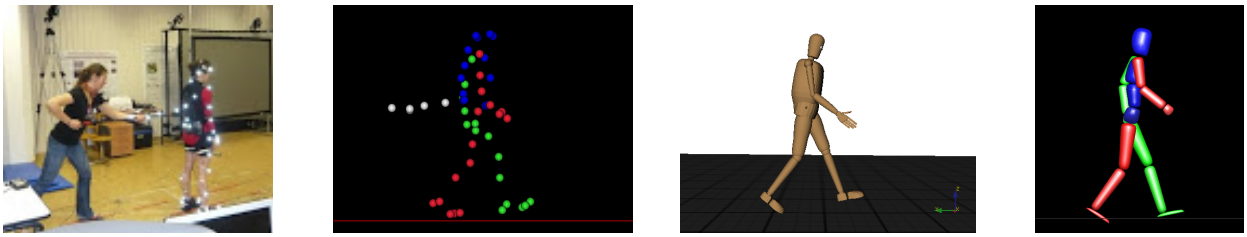

(a) (b) (c) (d)

Fig. 3: Overview of the conversion of the human motion to the joint angles used in the model: (a) Person and push device with markers for the motion capture procedure with Vicon, (b) Visualization of the marker position with Mokka, (c) Joint angles of the kinematic MMM model, (d) Motion of planar dynamical human model visualized with MeshUp.

positions of these points according to a coordinate system is saved as data files. The force of the disturbance is measured with a 3D force sensor from OptoForce [3]. Both, the motion and the push are recorded with a rate of 100 Hz. The motion kinetic and kinematic analyzer Mokka [2] can be used to visualize this data. At KIT the Master Motion Map (MMM) [1] has been developed. It was used to map the three dimensional position data of the markers to a kinematic model to calculate the joint angles. This data is converted to the planar human model based on `HeiMan` described in detail in SectionII-A which can be visualized with `MeshUp` [9]. Therefore it is important to ensure that the motion that is to be analyzed is mostly in sagittal plane.

We consider motions with disturbances from the back at different height and of various strength. During the experiments the probands were wearing a protector to secure from pain and injure. The influence of the tissue of the protector was neglected in our simulation. By the time of the experiments the pushed subject was 1.77 m tall, weighted 57 kg and of an age of 23 years.

III. COMPUTATIONAL RESULTS

The methods, described in the previous sections, are applied to motions with and without disturbances. We formulate the hypothesis that for stronger and higher located pushes the internal joint torques are higher. In this section four main results are presented.

- First, we analyze how well our solution fits the reference data.
- Second, the internal joint torques are compared with respect to the different joints and the location of the push point.
- Third, it is shown that there is no strict relation between a high variation in the joint angles and the internal joint torques.
- Forth, a first analysis of relevant quantities as integral means of joint torques, duration and step length, that could be use as objective functions for motion generation, is given.

For our analysis we consider seven motions of the same subject. Two undisturbed walking motions (referred to as 'NoPush') are taken into account to show that also these

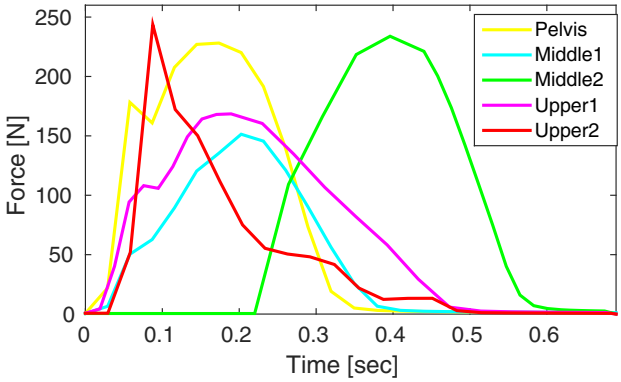

Fig. 4: Strength and duration of the disturbances for the five analyzed motions.

are not equal, but have a comparable shape. The pushes are applied at three different locations at the spine: at the pelvis, the middle and the upper trunk, see Figure 2. The pushes differ also in strength as well as in profile and in timing. They are applied from the back, which is the negative x-direction in our model. We model one single step. The start and duration of the disturbance does not vary a lot. In the considered motions the perturbation is applied during the swinging phase of the left leg: after the liftoff of the left hallux and before the touchdown of the left heel. An overview of the time dependent amplitude and the normalized force of the disturbances in the different motions is shown in Figure 4 and Table I.

As the model motion is very similar to the recorded motion of the human, we can transfer the results from the model to the human. In Table II in the first two columns the errors of the fit of the model to the reference motions is given. We calculate the root-mean squared (RMS) error for translational and rotational DoF separately:

$$err = \sqrt{\frac{1}{n_q m}\left[\sum_{k\in\mathscr{C}}\sum_{j=0}^{m}(q_k(t_j)-\tilde{q}_k(t_j))^2\right]}, \qquad (13)$$

where m is the total number of multiple shooting nodes of the optimal control problem and $\mathscr{C}$ is the set of indexes

TABLE I: Properties of the push and timing of the motion. The events in the graph on the right stand for 1: Push Start, 2: Right Heel Liftoff, 3: Push End, 4: Left Heel Touchdown, 5: Left Hallux Touchdown, 6: Right Hallux Liftoff.

Motion	Push Force (Maximum) [N]	Duration of Step [sec]	Push Start [sec]	Right Heel Liftoff [sec]	Push End [sec]	Left Heel Touchdown [sec]	Left Hallux Touchdown [sec]	Right Hallux Liftoff [sec]
NoPush1	0	0.730		0.38		0.60	0.73	0.79
NoPush2	0	0.670		0.40		0.53	0.67	0.69
Pelvis	227	0.610	0.09	0.26	0.35	0.53	0.61	0.62
Middle1	143	0.630	0.09	0.25	0.39	0.54	0.63	0.65
Middle2	223	0.530	0.22	0.37	0.48	0.52	0.53	0.58
Upper1	169	0.470	0.01	0.14	0.35	0.44	0.47	0.51
Upper2	247	0.500	0.05	0.22	0.32	0.46	0.50	0.52

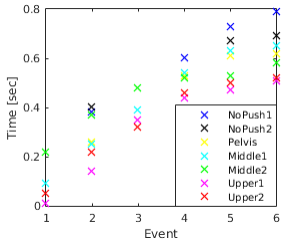

TABLE II: RMS errors of the motion fitting, step length and integral of squared torques for the different considered motions.

Motion	RMS error Translation [m]	RMS error Rotation [rad]	Step Length Before [m]	Step Length After [m]	Step Length Difference [m]	Squared Torques Legs [Nm^2]	Squared Torques Body [Nm^2]	Squared Torques Arms [Nm^2]
NoPush1	0.0127	0.0103	0.404	0.459	0.055	4770	239.05	19.42
NoPush2	0.0090	0.0138	0.468	0.507	0.039	2968	288.84	12.87
Pelvis	0.0137	0.0127	0.415	0.635	0.220	4289	144.98	30.99
Middle1	0.0198	0.0117	0.496	0.655	0.159	4689	218.78	6.28
Middle2	0.0134	0.0190	0.390	0.405	0.015	5939	116.70	64.29
Upper1	0.0235	0.0206	0.419	0.481	0.062	5009	220.17	38.86
Upper2	0.0361	0.0261	0.443	0.847	0.404	7258	211.48	68.15

belonging to the translational or rotational DoF. The translational RMS error varies between 0.009 and 0.0361 m and the rotational between 0.0103 and 0.261 rad. The values of the translations vary around 0.8 m and the rotational angles with around 1.2 rad. Therefore the error between the motion of the model and the reference data is very small. Interestingly the error is less for the disturbances at the pelvis than for the ones at the middle and upper trunk even if the push is stronger. This could be due to the fact that we approximate the 24 joints of the spine with only two joints.

The focus of this work lies in the analysis of the internal torques in the joints. They are constant on the time intervals coming from the discretization of the controls of the model as described in Section II-C The strength of the disturbance as well as the location of the push point have an influence on the set of joints with increased torques and their amplitude. There are some distinct differences for the different motions considered. For all but the motions without disturbances and the one with the lowest push the torques in both shoulders are higher in the middle of the step the more the motion is disturbed, see Figure 6 line four and five column one. The differences in the torques in the legs are not the same in both legs. In the stance leg (right) the torques in the ankle are higher at the point in time when the push ends for all disturbed motions compared with the motions without disturbances. For all disturbed motions but the one with push at the pelvis also the torque in the knee is higher. In the swing leg (left) there are only higher torques for the motions with pushes at the upper body. For strong pushes at the middle and upper trunk the torques in the head joint are higher than in the undisturbed walking motions.

Looking at the relation between the variation of the joint angles and the variation of the internal torques, the importance of our approach becomes clear. In most joints it can be observed that a higher internal torque results in a change of the joint angle velocity. But the opposite does not hold: For example in the left ankle a change in the velocity can be observed for the strong push at the upper body at $t = 0.5$ sec (see Figure 5 third line first column), but the torques are around 0 Nm, see Figure 6 third line second column. This observation can be due to the influence of the dynamics of the model that cannot be measured. Therefore it is important to be able to calculate the internal joint torques based on a model as presented in this paper.

As a motivation for future work, we analyze relevant quantities that can lead to valuable results for motion generation. For our approach of motion generation [16] an objective function is needed. A common approach is the minimization of the squared joint torques, meaning the control of our model, leading to energy minimal motions, the minimization of the duration of the step or the maximization of the step length. In general, the steps with disturbances are faster than the ones without disturbances, but there is no direct relation between the duration of the step and the force of the push: For the middle trunk the duration decreases for a stronger push, while for the upper trunk the duration increases, see Table I column two. Analyzing the step length, there is no direct relation between step length variation (between the step length at the beginning and the end of the motion) and the force strength or the point where the disturbance is applied, see also Table II column three to five. We calculated the squared internal of joint torques for different groups of joints (Legs: Hips, Knees, Ankles; Body: Lumbar, Thorax, Neck; Arms: Shoulders, Elbows). For the legs and the arms the assumption, that a stronger disturbance applied at a

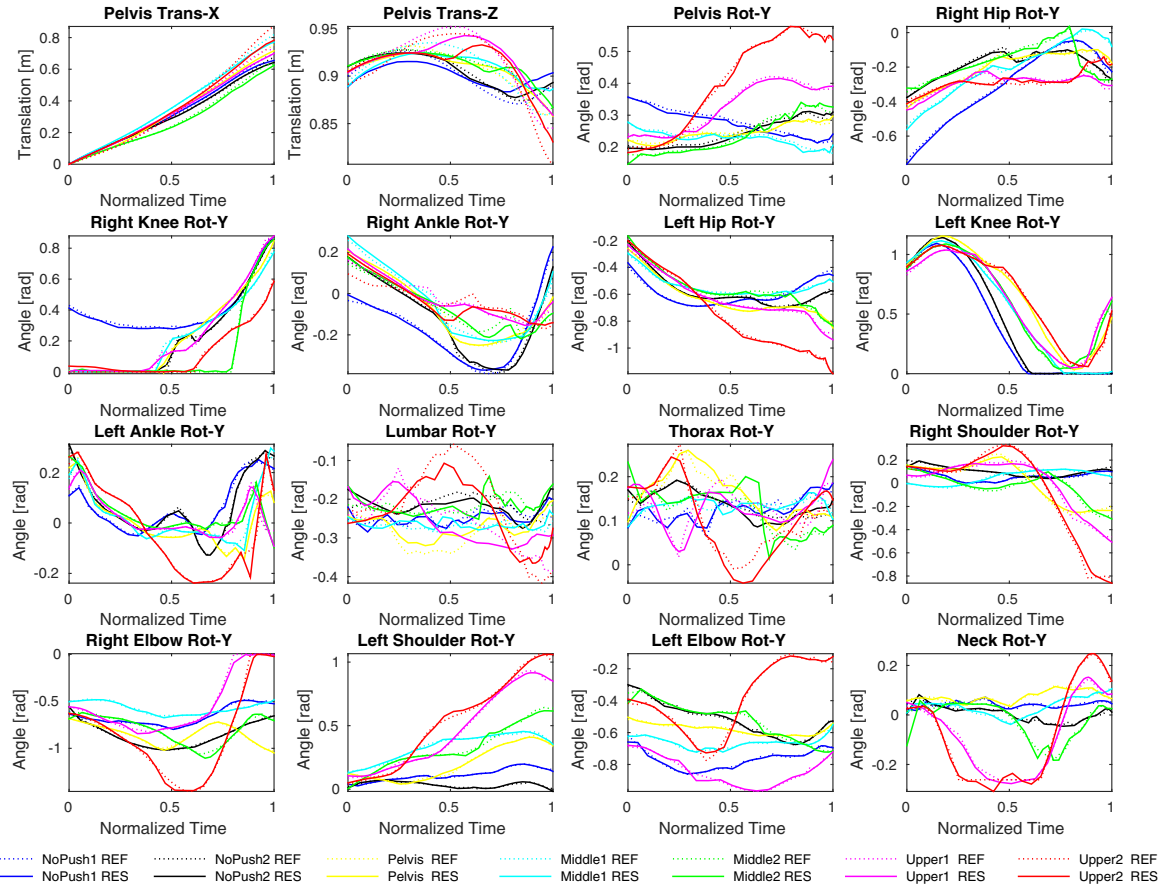

Fig. 5: Translation of the pelvis and joint angles of the reference data (dotted lines) and the model (solid lines) for the seven analyzed motions.

higher point at the spine results in higher torque integral, holds. Interestingly, this assumption does not hold for the body: A stronger push results in a lower torque integral for the pushes in the middle and the upper trunk, while the torque integral still increases the higher the disturbance is located at the spine, see also Table II column six to eight.

All in all our assumption: "the stronger the disturbance and the higher the push point is located at the spine, the higher the torques in the joints" holds. Note, that further research with a wider range of motions is necessary to gain results that can be seen as general rule.

IV. CONCLUSION AND OUTLOOK

In this work an optimization based simulation approach to obtain the internal joint torques during disturbed walking motion of a human is presented. A planar model is included into an optimal control problem that minimizes the difference between the joint angles of the reference data and the joint angles of the model to obtain a motion that fulfills the constraints of the model and represents the dynamics. Additional a description of how to implement external perturbations and an overview of the optimization algorithms used for the forward dynamics optimization is given. Furthermore the recording of the motion capture data is described. The motion resulting from a motion fitting optimization to this data leads to a good approximation of this reference data. With a model as considered in this work it is possible to gather data, that is hard to get from a real human, as the center of mass, and data, that is impossible to calculate with a kinematic model, as the calculation of ground reaction forces.

In future work we plan to investigate for more push recovery motions of more than one subject with a larger variety of pushes and to analyze more potential objective functions, extend the model to allow for multiple steps and pushes from different direction (3D model), as well as to improve the modeling of the spine to get even better approximations of disturbed motions. We will also follow the approach of motion generation from [16] using a variety of objective functions, e.g. minimization of time or maximization of step length, use inverse optimal control to identify the weights of these criteria, which lead to human like motions, [6] and apply the presented optimal control framework to dynamic robot models (HRP2/HeiCub) to compute optimal recovery motions and recovery primitives, [13].

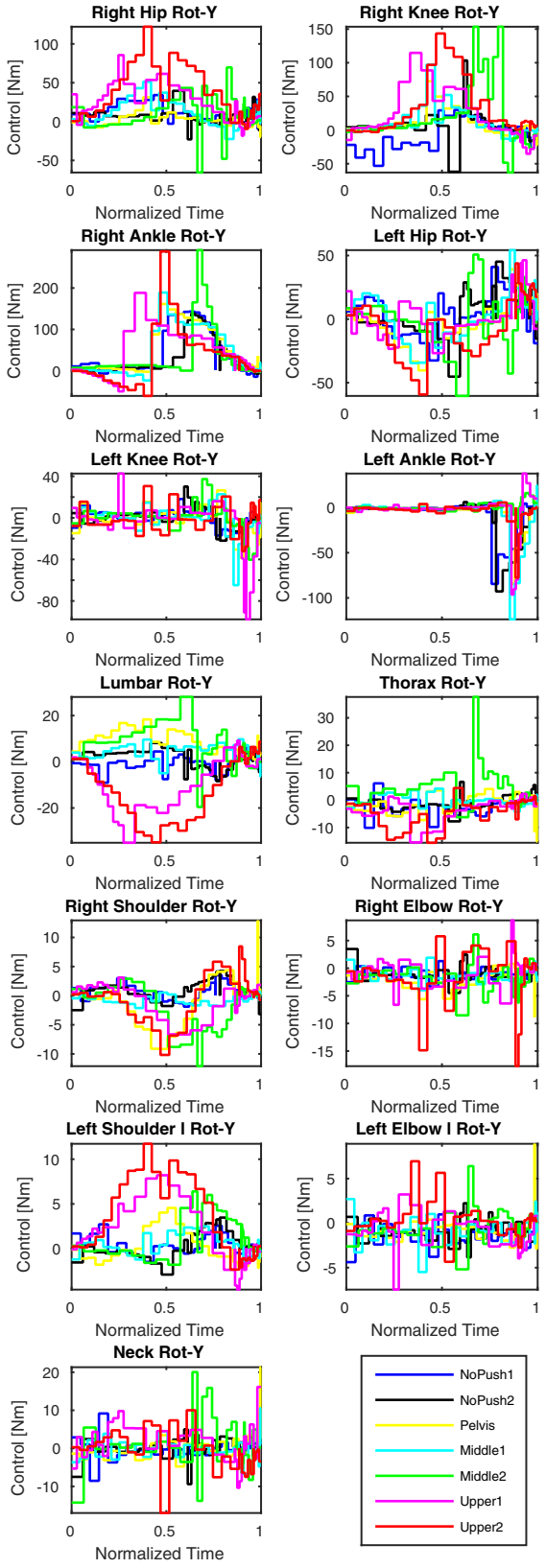

Fig. 6: Internal torques in the joints of the model for the seven analyzed motions.

ACKNOWLEDGMENT

We want to thank the Simulation and Optimization research group of the IWR at Heidelberg University for giving us the possibility to work with MUSCOD-II. We also want to thank T. Asfour and co-workers, KIT, Karlsruhe for providing the MMM framework.

REFERENCES

[1] MMM - Master Motor Map. http://mmm.humanoids.kit.edu/index.html. Accessed: 29 February 2016.

[2] Mokka. https://b-tk.googlecode.com/svn/web/mokka/index.html. Accessed: 29 February 2016.

[3] Optoforce sensor. http://optoforce.com/wp-content/uploads/2014/05/OMD-30-SC-600N-DATASHEET.pdf. Accessed: 29 February 2016.

[4] Vicon Motion Capture. http://www.vicon.com/. Accessed: 29 February 2016.

[5] H.G. Bock and K.J. Plitt. A multiple shooting algorithm for direct solution of optimal control problems. pages 243–247. Pergamon Press, 1984.

[6] D. Clever and K. Mombaur. On the relevance of common humanoid gait generation strategies in human locomotion - an inverse optimal control approach. In H.G. Bock, X.P.and Rannacher Hoang, and J. R., Schlöder, editors, *submitted to Modeling, Simulation and Optimization of Complex Processes - HPSC 2015*, page 12 pages. Springer, 2015.

[7] M. L. Felis. *Modeling Emotional Aspects in Human Locomotion*. PhD thesis, Heidelberg University, 2015.

[8] M. L. Felis. Rbdl - an efficient rigid-body dynamics library using recursive algorithms. *Autonomous Robots*, 2015, submitted.

[9] M. L. Felis. Meshup - visualization tool for multibody systems based on skeletal animation, 2016. Accessed: 29 February 2016.

[10] M. L. Felis, K. Mombaur, and A. Berthoz. Mathematical modeling of emotional body language during human walking. In H. G. Bock, X. P. Hoang, R. Rannacher, and J. P. Schlöder, editors, *Modeling, Simulation and Optimization of Complex Processes - HPSC 2012*, pages 25–35. Springer International Publishing, 2014.

[11] M. L. Felis, K. Mombaur, and A. Berthoz. An optimal control approach to reconstruct human gait dynamics from kinematic data. In *IEEE/RAS International Conference on Humanoid Robots (Humanoids 2015)*, 2015.

[12] B. Hwang and D. Jeon. A method to accurately estimate the muscular torques of human wearing exoskeletons by torque sensors. *Sensors*, pages 8337–8357, 2015.

[13] K.H. Koch, D. Clever, K. Mombaur, and D. Endres. Learning movement primitives from optimal and dynamically feasible trajectories for humanoid walking. In *Humanoid Robots (Humanoids), 2015 15th IEEE-RAS International Conference on*, pages 866–873. IEEE, 2015.

[14] D. B. Leineweber, I. Bauer, H.G. Bock, and J.P. Schlöder. An efficient multiple shooting based reduced SQP strategy for large-scale dynamic process optimization - Part I: theoretical aspects. pages 157 – 166. 2003.

[15] E. C. Martinez-Villalpando and H. Herr. Agonist-antagonist active knee prosthesis: A preliminary study in level-ground walking. *Journal of Rehabilitation Research and Development*, pages 361–374, 2009.

[16] R. M. Schemschat, D. Clever, M. L. Felis, and K. Mombaur. Optimal push recovery for periodic walking motions. *submitted to 6th IFAC International Workshop on Periodic Control Systems*, 2016.

[17] B. Stephens. Humanoid push recovery. *7th IEEE-RAS International Conference on Humanoid Robots*, pages 589–595, 2007.

[18] K.-Y. Tu and W.-C. Lee. Analysis and study of human joint torque and motion energy during walking on various grounds. In *Communications in Computer and Information Science*, pages 73–81, 2010.

[19] A. Wit and A. Czaplicki. Inverse dynamics and artificial neural network applications in gait analysis of the disabled subjects. In *Human Movement*, pages 93–102, 2008.

[20] S.-J. Yi, B.-T. Byoung-Tak Zhang, Hong D., and D. D. Lee. Online learning of a full body push recovery controller for omnidirectional walking. *2011 11th IEEE-RAS International Conference on Humanoid Robots*, 2011.